INTEGRAL BROADBAND SPECTROSCOPY OF VELA X-1

P. Kretschmar[1,3], **R. Staubert**[2], **I. Kreykenbohm**[2,3], **M. Chernyakova**[3], **A. v. Kienlin**[1], **S. Larsson**[4],
K. Pottschmidt[1,3], **J. Wilms**[2,5], **L. Sidoli**[6], **A. Santangelo**[7], **A. Segreto**[7], **D. Attie**[8], **P. Sizun**[8], and **S. Schanne**[8]

[1]Max-Planck-Institut für Extraterrestrische Physik, 87548 Garching, Germany
[2]Institut für Astronomie und Astrophysik – Astronomie, Univ. of Tübingen, 72076 Tübingen, Germany
[3]INTEGRAL Science Data Center, 1290 Versoix, Switzerland
[4]Department of Astronomy, Stockholm University, SE-10691 Stockholm, Sweden
[5]Department of Physics, University of Warwick, CV4 7AL Warwick, UK
[6]Istituto di Astrofisica Spaziale e Fisica Cosmica – CNR, 20133 Milano, Italy
[7]Istituto di Astrofisica Spaziale e Fisica Cosmica – CNR, 90146 Palermo, Italy
[8]Service d'Astrophysique, CEA–Saclay, 91191 Gif-sur-Yvette, France

ABSTRACT

The wind-accreting X-ray binary pulsar and cyclotron line source Vela X-1 has been observed extensively during *INTEGRAL* Core Program observations of the Vela region in June-July and November-December 2003. In the latter set of observations the source showed intense flaring – see also Staubert et al. (2004), these proceedings.

We present early results on time averaged and time resolved spectra, of both epochs of observations. A cyclotron line feature at $\sim$53 keV is clearly detected in the *INTEGRAL* spectra and its broad shape is resolved in *SPI* spectra. The remaining issues in the calibration of the instruments do not allow to resolve the question of the disputed line feature at 20-25 keV.

During the first main flare the average luminosity increases by a factor of $\sim$10, but the spectral shape remains very similar, except for a moderate softening.

Key words: Vela X-1; INTEGRAL; cyclotron lines.

1. INTRODUCTION

Vela X-1 (4U 0900−40) is an eclipsing high mass X-ray binary with an orbital period of 8.96437 days (Barziv et al. 2001) at a distance of $\sim$2.0 kpc (Nagase 1989) consisting of the B0.5Ib supergiant HD 77581 and a neutron star. The optical companion has a mass of $\sim$23 $M_\odot$ and a radius of $\sim$30 $R_\odot$ while the neutron star mass is estimated to be $\sim$1.8$M_\odot$ (Barziv et al. 2001).

Due to the small separation of the binary system (orbital radius: 1.7 $R_\star$), the neutron star is deeply embedded in the intense stellar wind (4×10^{-5} $M_\odot$/yr; Nagase et al. 1986) of HD 77581. X-ray line spectra measurements (Sako et al. 1999) show that this wind is inhomogeneous with dense clumps embedded in a much thinner, highly ionized component. The typical X-ray luminosity of Vela X-1 is $\sim$4$\times10^{36}$ erg/s, but both sudden flux reductions to less than 10 % of its normal value (Inoue et al. 1984; Lapshov et al. 1992; Kreykenbohm et al. 1999) and flaring activity (Kendziorra et al. 1990; Haberl & White 1990; Kreykenbohm et al. 1999) have been observed in the past.

The neutron star has a spin period of $\sim$283 s (McClintock et al. 1976). Both spin period and period derivative have changed erratically since the first measurement as is expected for a wind accreting system. The last measurements with the Burst and Transient Source Experiment[1] resulted in a period of $\sim$283.5 s.

The broadband X-ray spectrum of Vela X-1 has the typical shape of accreting pulsar spectra with a power law continuum at lower and an exponential cutoff at higher energies. This is further modified by strongly varying absorption which depends on the orbital phase of the neutron star (Kreykenbohm et al. 1999; Haberl & White 1990), an iron fluorescence line at 6.4 keV, and occasionally an iron edge at 7.27 keV (Nagase et al. 1986). A cyclotron resonant scattering feature (CRSF) at $\sim$55 keV was first reported from observations with *Mir-HEXE* (Kendziorra et al. 1992). Makishima et al. (1992) and Choi et al. (1996) reported an absorption feature at $\sim$25 keV to 32 keV from *Ginga*. This lower energy feature has been disputed by *BeppoSAX* observations (Orlandini et al. 1998) but supported by phase resolved analysis of *Mir-HEXE* (Kretschmar et al. 1997) and *RXTE* data (Kreykenbohm et al. 2002).

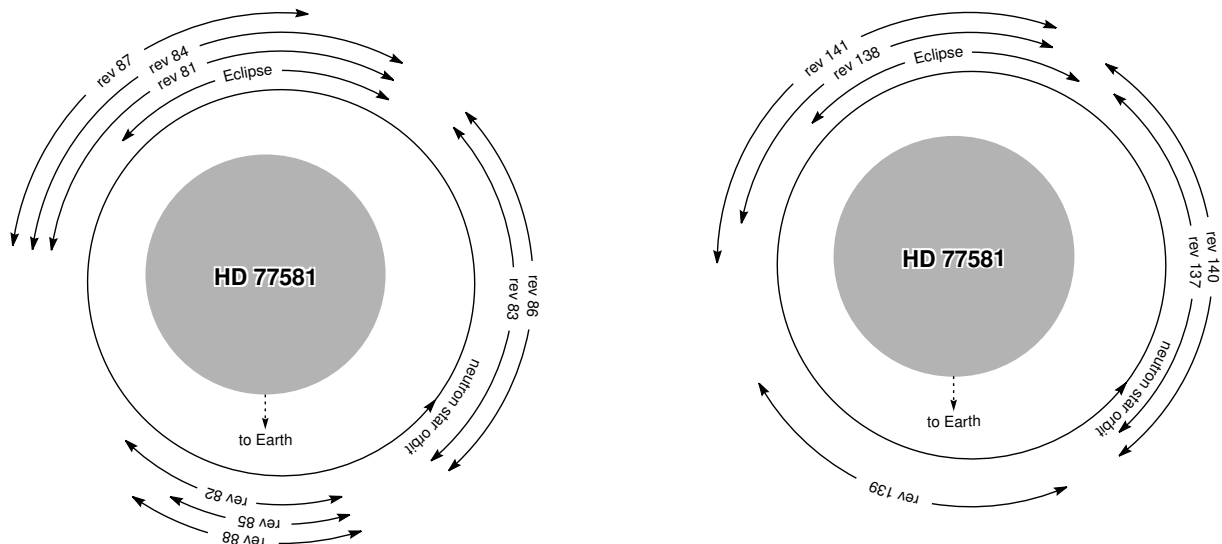[1]See `http://www.batse.msfc.nasa.gov/batse/pulsar/data/sources/velax1.html`

Figure 1. Sketch of the Vela X-1 System during the observations in summer and in winter 2003. The source position along its orbit during the INTEGRAL observations is indicated for each INTEGRAL revolution.
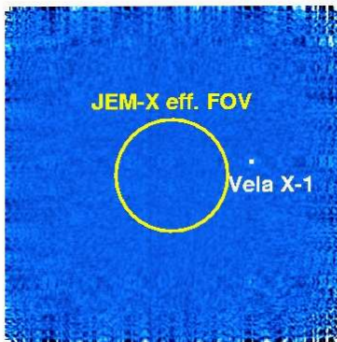

Figure 2. ISGRI image of pointing 013700420010 during which the first major Vela X-1 flare reached its peak. The source was outside of the field of view of the monitor instruments.

2. OBSERVATIONS AND DATA REDUCTION

As part of the *INTEGRAL* Core Program the Vela region has been observed twice in 2003 for an extended time. The first set of observations took place mid June to early July (revolutions 81 to 88) the second end of November to mid December (revolutions 137 to 141).

As the observations were not targeted at any specific source in order to support different scientific goals, the observation strategy was not optimized for Vela X-1. In practice this meant that several revolutions were scheduled with Vela X-1 in eclipse (see Fig. 1) and that for a significant fraction of the time the source was not within the field-of-view of the two monitor instruments *JEM-X* and *OMC*.

The two observation epochs, summer and winter, saw a very different behaviour of Vela X-1. While in summer the source was mostly calm, the winter observa-

tions showed several large flares (Krivonos et al. 2003; Staubert et al. 2004), possibly the largest ever observed. These flares and the general source behaviour during the observations are described in more detail in Staubert et al. (2004). Unfortunately the observation strategy explained above means that we have no coverage for the flares with the monitor instruments. Also the *RXTE-ASM* did not sample this source region during the flares.

For the summer observations we exctracted long term average spectra for all three high energy instruments, excluding times of eclipse and pointings with other problems like, e.g., radiation belt entries. While these spectra only describe an average source state and the exact selection varies from instrument to instrument, the large total exposure allows to determine a statistically significant SPI spectrum beyond $50\,\mathrm{keV}$ despite the steeply falling source spectrum and degradation of the data by a large solar flare which occured in revolutions 82/83. The total integration times for the combined spectra are 340.2 and 333.2 ksec for *JEM-X* and *ISGRI*, respectively, where concurrent observations were chosen and 775.6 ksec for *SPI*.

For the winter observations we have concentrated on the spectra before and during the first big flare. In this case we have generated pulse phase resolved spectra covering the rise, the peak and falling flank and the following off-pulse region connected with the so-called "main pulse" as defined, e.g., by Kreykenbohm et al. (2002). The used bins are indicated in Fig. 3.

The data reduction was done with the *OSA 3* release of the scientific analysis software and the corresponding calibration files. Due to the remaining problems in the *ISGRI* response matrix with "snake-like" residuals, we assumed systematic uncertainties of 10% for the extracted *ISGRI* spectra. For *JEM-X* a known problem exists in reconstructing fluxes below $\sim\!10\,\mathrm{keV}$, in our case this leads to artificially enhanced intrinsic absorption in the, typically strongly absorbed, source.
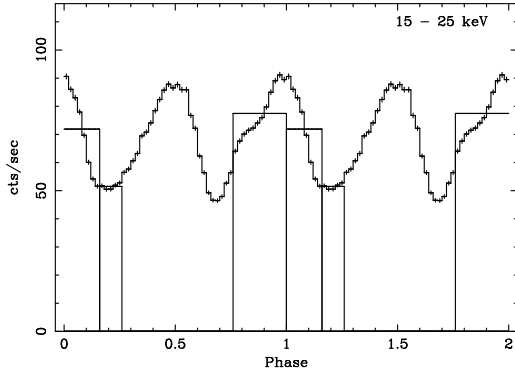
Figure 3. The phase intervals chosen for the pulse phase resolved spectroscopy.

Since no direct support for pulse phase resolved analysis is yet available in the analysis software, we constructed specific GTI information for the different phase bins. These GTIs are based on the barycenter and binary corrected pulse period determination (Staubert et al. 2004) from which then times in the instrumental time frame were derived.

3. RESULTS

The combined spectra of *JEM-X* and *SPI* for the summer observations can be well fitted at lower energies by a power law model with exponential cutoff (*XSPEC* model `CUTOFFPL`), if one includes free relative normalization between the two spectra, to allow for (inter-)calibration uncertainties. A powerlaw with a Fermi-Dirac cutoff (Tanaka 1986) works equally well and gives very similar results, but the onset of the cutoff is not well determined, thus we use the simpler model here.

Above 50 keV there is an evident structure in the fit residuals for *SPI*, see Fig. 4. This structure can be fitted by including a cyclotron scattering feature at $E \approx 54$ keV with $\sigma \approx 7$ keV. Since the SPI energy resolution at these energies is ~ 1.6 keV (Attié et al. 2003), the line shape can actually be resolved as far as statistics permit it. The line parameters do not depend siginificantly on the exact continuum – simple exponential cutoff or Fermi-Dirac cutoff – used.

Combining *JEM-X* and *ISGRI* spectra, the missing flux above ~ 50 keV is again clearly visible in the fit residuals – see Fig. 5 – and can be fitted with a line at $E \approx 52$ keV. Combining spectra from all three high energy instruments does not allow a good fit due to calibration differences between *ISGRI* and *SPI* even though the fit parameters are mostly compatible (see Tab. 1).

Unfortunately, the current calibration and cross-calibration uncertainties for the *INTEGRAL* instruments do not allow any firm statement about the existence or not of a ~ 25 keV line in the spectra. All spectral modeling has been done without including such a feature but a feature of the strength reported, e.g., by Kreykenbohm et al. (2002) would be fully consistent with the data at the moment.
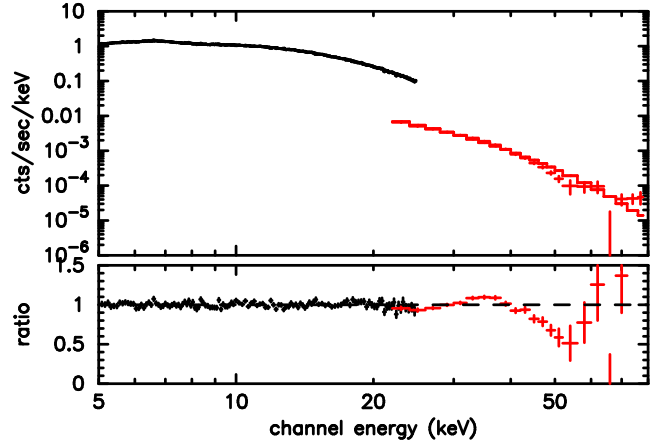

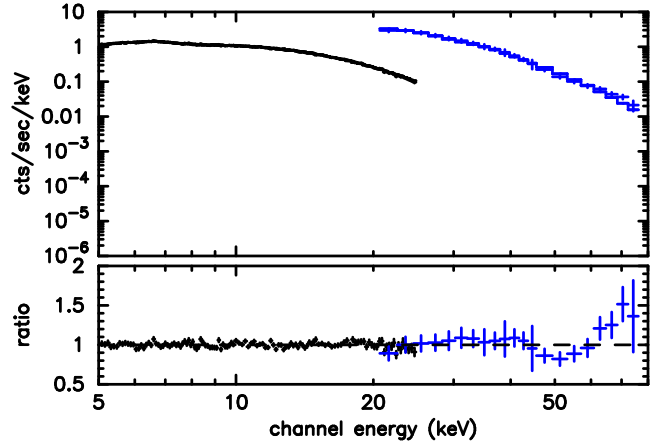*Figure 4. Combined JEM-X and SPI spectra averaged over the good pointings during the summer observations.*

Figure 5. Combined JEM-X and ISGRI spectra averaged over the good pointings during the summer observations.

Table 1. Selected best fit parameters for the combined, phase averaged JEM-X & SPI spectra and JEM-X & ISGRI spectra respectively using the XSPEC `CUTOFFPL` *model. Note that the values are still preliminary due to calibration uncertainties.*

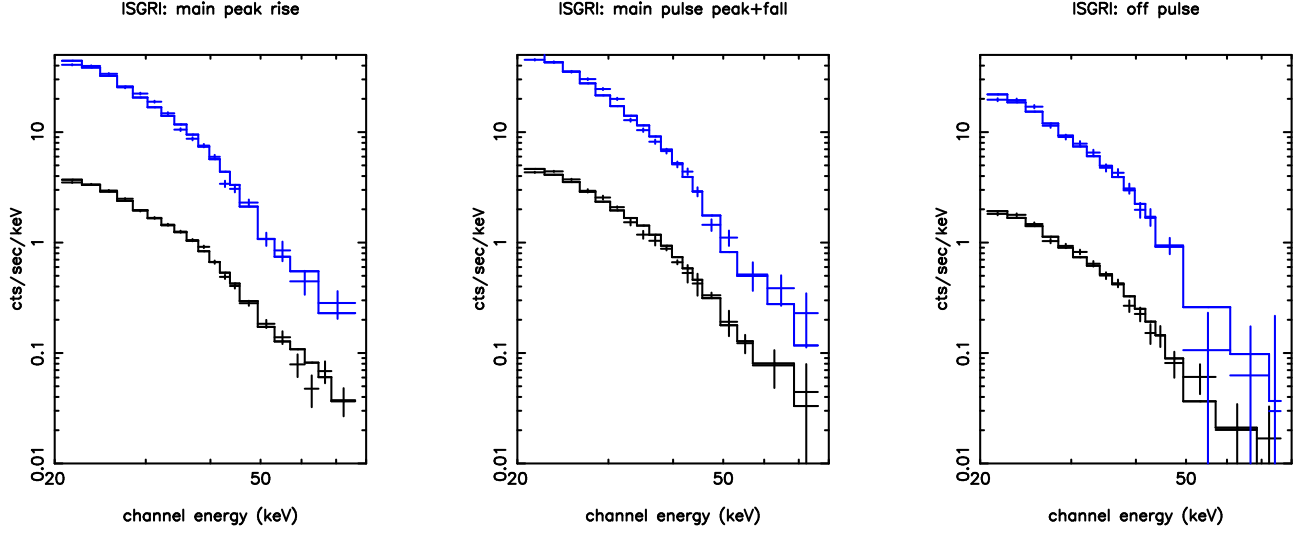| Parameter	JEM-X + SPI	JEM-X + ISGRI
photon index	$0.51^{+0.10}_{-0.20}$	$0.43^{+0.10}_{-0.16}$
folding energy	$11.3^{+0.7}_{-1.3}$ keV	$12.1^{+0.9}_{-0.6}$ keV
line center	$53.6^{+3.4}_{-1.8}$ keV	$51.9^{+2.4}_{-2.6}$ keV
line σ	$7.3^{+1.8}_{-1.3}$ keV	$4.0^{+3.5}_{-3.7}$ keV
line depth	$0.63^{+0.13}_{-0.08}$	$0.38^{+\infty}_{-0.16}$
$\chi^2_{\rm red}$ with line	1.19	1.02
$\chi^2_{\rm red}$ w/o line	1.85	1.17

Figure 6. Comparison of ISGRI spectra before and during the first large flare of Vela X-1. From left to right the panels show the spectra for the rising flank of the main pulse, the peak and falling flank and the following off-pulse region. In each panel the lower spectrum is that of the pre-flare while the upper is taken over the flare. The spectral softening is directly visible.

Table 2. Selected best fit parameters for phase resolved ISGRI spectra before and during the large flare of Vela X-1 in revolution 137, using the XSPEC `CUTOFFPL` model. Note that the best fit values are still preliminary.

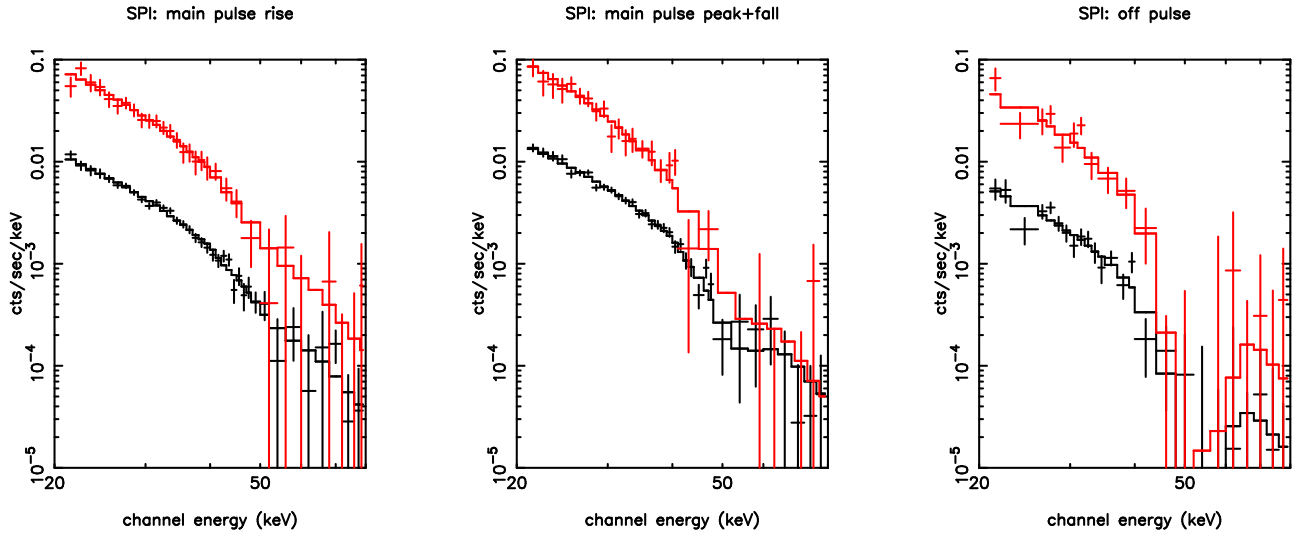| Parameter	Main pulse rise		Main pulse peak & fall		Off pulse	
	pre-flare	flare	pre-flare	flare	pre-flare	flare
norm	$0.13^{+0.01}_{-0.01}$	$2.14^{+0.62}_{-0.05}$	$0.21^{+0.03}_{-0.02}$	$2.88^{+0.09}_{-0.07}$	$0.09^{+0.03}_{-0.01}$	$1.43^{+0.25}_{-0.29}$
folding energy	$11.2^{+0.5}_{-0.3}$ keV	$9.6^{+0.1}_{-0.6}$ keV	$10.0^{+0.5}_{-0.3}$ keV	$8.9^{+0.1}_{-0.1}$ keV	$9.6^{+0.4}_{-0.7}$ keV	$8.5^{+0.6}_{-0.3}$ keV

Figure 7. Comparison of SPI spectra before and during the first large flare of Vela X-1. The panels follow the same pattern as in Fig. 6. Due to the relatively short integration times, the feature at ~50 keV is not clearly visible.

Table 3. Selected best fit parameters for phase resolved SPI spectra before and during the large flare of Vela X-1 in revolution 137, using the XSPEC `CUTOFFPL` model. Note that the best fit values are still preliminary.

Parameter	Main pulse rise		Main pulse peak & fall		Off pulse	
	pre-flare	flare	pre-flare	flare	pre-flare	flare
norm	$0.25^{+0.05}_{-0.04}$	$2.17^{+0.81}_{-0.58}$	$0.32^{+0.07}_{-0.05}$	$4.16^{+2.50}_{-1.56}$	$0.13^{+0.09}_{-0.05}$	$1.59^{+2.10}_{-0.90}$
folding energy	$11.4^{+0.8}_{-0.8}$ keV	$10.2^{+1.1}_{-1.0}$ keV	$11.5^{+0.8}_{-0.8}$ keV	$8.3^{+1.2}_{-1.0}$ keV	$11.0^{+2.5}_{-1.8}$ keV	$9.6^{+3.3}_{-2.1}$ keV

3.1. Winter observations

For the pre-flare and flare data of the winter observations we are restricted to spectra from the two main instruments as explained in Section 2. Fig. 6 and Fig. 7 show for comparison the phase resolved spectra of before and during the first big flare. While the flux increases by a factor of about 10 during the flare, the spectral shape stays more or less the same, except for a certain softening, which is directly visible in the count spectra.

Using the same model as for the summer observations the folding energy parameter, which can be seen as a measure of temperature, decreases by 1–1.5 keV during the flare, see Tab. 2 and Tab. 3. For these fits the photon index of the continuum and the line width and energy were ill determined and fixed to the values found for the summer data, see Tab. 1. This had little effect on the continuum parameters.

4. DISCUSSION

While the remaining uncertainties in the calibration of the individual instruments as well as in the intercalibration do not allow any firm statement about a possible line feature at 20-25 keV we clearly observe and resolve – thanks to the high spectral resolution of *SPI*– the well-known line feature above 50 keV. The half-width of $7.2^{+1.5}_{-1.2}$ keV obtained from *SPI* data is in the typical range of line widths reported from observations with other instruments and expected from thermal broadening. It falls inbetween the relatively narrow line solution reported by Coburn et al. (2002) and the very broad line width given in Orlandini et al. (1998). It should also be kept in mind that this line width is obtained for a long-term time averaged spectrum, as for shorter integration times the statistics do not allow to constrain the fluxes in this energy range anymore.

Based on the theoretical cyclotron line shapes proposed, e.g., by Araya & Harding (1999), the broad, flat shape and lack of additional structure could be taken as indication that this line is indeed a harmonic and not the more structured fundamental. Alternatively, this would indicate observation at a relatively narrow angle to the magnetic field and preferably of a cylindrical emission region.

It is interesting to see that despite a rapid, strong brightening, the source spectrum appears to remain very similar to that obtained during more ususal flux levels. With a normal luminosity of $\sim 4 \times 10^{36}$ ergs/s the wind-accreting source remains in the sub-Eddington regime of accretion even during the flares. Given the well known pulse to pulse variations (Staubert et al. 1980) one can speculate that the normal mode of accretion for Vela X-1 is a relatively sparse and inhomogenous flow which does not fill the accretion column completely. In this picture the spectral softening observed could be caused by additional comptonisation of X-ray photons by a more densely filled accretion column.

A more detailed analysis of this extensive and higly interesting dataset than can be done for these proceedings is surely called for in the future. With further improved flux reconstruction and calibration information not only the question of the 20-25 keV line can be settled but we will also arrive to do detailed quantitative studies of the spectral evolution in calm and flaring times.

REFERENCES

Araya R.A., Harding A.K.1999, ApJ, 517, 334

Attié D., Cordier B., Gros M., et al.2003, A&A, 411, L71

Barziv O., Kaper L., Van Kerkwijk M.H., Telting J.H., Van Paradijs J.2001, A&A, 377, 925

Choi C.S., Dotani T., Day C.S.R., Nagase F.1996, ApJ, 471, 447

Coburn W., Heindl W.A., Rothschild R.E., et al.2002, ApJ, 580, 394

Haberl F., White N.1990, ApJ, 361, 225

Inoue H., Ogawara Y., Ohashi T., et al.1984, PASJ, 36, 709

Kendziorra E., Mony B., Maisack M., et al.1990, In: Proc. of the 23rd ESLAB Symposium on Two Topics in X-ray Astronomy, ESA SP-296, (1)467–471, ESA Publications Division

Kendziorra E., Mony B., Kretschmar P., et al., 1992, In: Tanaka Y., Koyama K. (eds.), Frontiers of X-Ray Astronomy, Frontiers Science Series 2, Tokyo, 51–52

Kretschmar P., Pan H.C., Kendziorra E., et al.1997, A&A, 325, 623

Kreykenbohm I., Kretschmar P., Wilms J., et al.1999, A&A, 341, 141

Kreykenbohm I., Coburn W., Wilms J., et al.2002, A&A, 395, 129

Krivonos R., Produit N., Kreykenbohm I., et al.2003, The Astronomer's Telegram, 211, 1

Lapshov I.Y., Sunyaev R.A., Chichkov M.A., et al.1992, Sov. Astron. Lett., 18, 16

Makishima K., Mihara T., Nagase F., Murakami T., 1992, In: Tanaka Y., Koyama K. (eds.), Frontiers of X-Ray Astronomy, Frontiers Science Series 2, Tokyo,, 23–32

McClintock J., Rappaport S., Joss P., et al.1976, ApJ, 206, L99

Nagase F.1989, PASJ, 41, 1

Nagase F., Hayakawa S., Sato N.1986, PASJ, 38, 547

Orlandini M., Dal Fiume D., Frontera F., et al.1998, A&A, 332, 121

Sako M., Liedahl D.A., Kahn S.M., Paerels F.1999, ApJ, 525, 921

Staubert R., Kendziorra E., Pietsch W., et al.1980, ApJ, 239, 1010

Staubert R., Kreykenbohm I., Kretschmar P., et al.2004, In: The INTEGRAL Universe, no. SP-552 in ESA, ESA Publications Division, ESTEC, Noordwijk, The Netherlands

Tanaka Y.1986, In: Mihalas D., Winkler K. (eds.) Radiation Hydrodynamics in Stars and Compact Objects, 198–221, Springer-Verlag, Berlin